1

Influence line- model correction approach for the assessment of engineering structures using novel monitoring techniques

Alfred Strauss[*1], Roman Wendner[1], Dan M. Frangopol[2] and Konrad Bergmeister[1]

*[1]Department of Civil Engineering and Natural Hazards, University of Natural Resources and
Life Sciences, Vienna, A-1190, Austria*
*[2]Department of Civil and Environmental Engineering, ATLSS Engineering Research Center, Lehigh Univ.,
117 ATLSS Dr., Bethlehem, PA 18015-4729, USA*

Abstract. In bridge engineering, maintenance strategies and thus budgetary demands are highly influenced by construction type and quality of design. Nowadays bridge owners and planners tend to include life-cycle cost analyses in their decision processes regarding the overall design trying to optimize structural reliability and durability within financial constraints. Smart permanent and short term monitoring can reduce the associated risk of new design concepts by observing the performance of structural components during prescribed time periods. The objectives of this paper are the discussion and analysis of influence line or influence field approaches in terms of (a) an efficient incorporation of monitoring information in the structural performance assessment, (b) an efficient characterization of performance indicators for the assessment of structures, (c) the ability of optimizing the positions of sensors of a monitoring system, and (d) the ability of checking the robustness of the monitoring systems applied to a structure. The proposed influence line- model correction approach has been applied to an integrative monitoring system that has been installed for the performance assessment of an existing three-span jointless bridge.

1. Introduction

In recent years major advances have been accomplished in the design, modeling, analysis, monitoring, maintenance and rehabilitation of civil engineering structures (Bergmeister *et al.* 2010, Frangopol 2011). These developments are considered to be at the heart of civil engineering, which is currently undergoing a transition towards a life-cycle and performance oriented design (Frangopol *et al.* 2008b). Monitoring is a key factor in this transition process, while the term "monitoring" includes all types of acquisition, observation and supervision of an activity or a process.

There is a large interest from scientists and practitioners in the investigation and development of monitoring systems and approaches for the efficient incorporation of monitored information in the performance assessment of structures associated with the identification of defects and degradation

---

Corresponding author, Associate professor, E-mail: alfred.strauss@boku.ac.at

processes (Bergmeister *et al.* 2010, Doebling *et al*. 1996, Messervey and Frangopol 2009, Strauss *et al.* 2009a, Frangopol 2011, Geier 2010, Inaudi 2010, Wenzel and Egerer 2010, Zilch et al. 2009). Promising statistical and analytical models (Messervey *et al.* 2010, Strauss *et al.* 2008a, Frangopol 2011) have been already developed for the optimization of monitoring periods (Kim and Frangopol 2010, Strauss *et al*. 2008b, Strauss *et al*. 2011, Kim and Frangopol 2011a, Frangopol 2011) and the incorporation of monitoring information in the performance assessment and the lifetime prediction of structures (Messervey *et al*. 2009, Frangopol 2011, Dorvash *et al.* 2010).

For instance, the American Society of Civil Engineers (ASCE) "Technical Council on Life-Cycle Performance, Safety, Reliability and Risk of Structural Systems" Task Group 2: "Reliability-Based Structural System Performance Indicators" characterized structural performance indicators that can be derived from a few structural quantities as essential parameters for effective maintenance planning. These indicators must guarantee the compliance with a series of design codes or general specifications (Frangopol *et al.* 2008, Strauss *et al.* 2011).

In general, monitoring methods are very suitable for the performance assessment (e.g., with respect to design codes or general specifications) of the region in the vicinity of the sensors but not for the entire structure, and hence cannot simply meet the characteristics of performance indicators as defined by the ASCE Technical Council on Life-Cycle Performance, Safety, and Reliability and Risk of Structural Systems.

A pairing of sensor readings with associated loading information (e.g., temperature or proof load magnitudes and its geometric coordinates) by influence line or influence field approaches provides the required sensor information for adjusting the model to existing behavior, using novel model correction approaches. Consequently, the sensor readings and the numerical performance of the adjusted model allow a comprehensive performance assessment with respect to code specifications and allow the definition of performance indicators in conjunction with monitoring processes or model correction quantities.

The objectives of this paper are the discussion and analysis of influence line or influence field approaches in terms of (a) an efficient incorporation of monitoring information in the structural performance assessment, (b) an efficient characterization of performance indicators for the assessment of structures, (c) the ability of optimizing the positions of sensors of a monitoring system, and (d) the ability of checking the robustness of the monitoring systems applied to a structure. In addition, the model correction approach, which is a key ingredient in the assessment procedures, and its properties are presented. The proposed influence line- model correction approach is discussed using the integrative monitoring system that has been installed for the performance assessment of an existing three-span joint less bridge structure.

2. Monitoring based modeling

There are numerous national and international regulations and publications which indicate the necessity of simulating the phenomena or event to be monitored. Simulations can contribute significantly to explaining the structural behavior in a comprehensive way, and serve for the detection of critical elements or regions. They can significantly support (a) the analysis of measurement uncertainties, (b) the experience for simulation procedures, and (c) the optimization of the monitoring layout. The simulation of phenomena to be monitored is considered by many engineers and researchers as a basis for an optimal monitoring layout and minimizing monitoring

uncertainties (RVS 13.03.11). The ability to correctly map monitoring quantities to structural characteristics by either numerical or analytical models is essential for the success of updating and identification strategies in general and the proposed influence line- and model correction approach in particular. Several aspects must be taken into account in modeling. The effort in the simulation and analysis (e.g., the use of 2D and 3D software tools) is determined by the complexity of the real structural behavior that has to be captured under variable loading conditions.

In structural engineering simulation techniques range from (a) efficient simplified static calculation techniques to (b) highly sophisticated nonlinear calculation techniques which are taking into account the overall system deformation and material laws.

Software packages such as ATENA (Červenka *et al.* 2007) provide advanced highly nonlinear material laws that can accurately represent existing material properties.

The application of the finite element method for capturing the real system behavior requires a careful discretization of the structure into macro- and finite elements. A proper selection of element type, element size and number of finite elements is highly important (Bathe 1995). The discretization must guarantee the detection of significant structural regions, such as areas of high strain and stress distributions and strain and stress gradients (Mayr and Thalhofer 1993). The knowledge about these areas is essential for the optimization of monitoring systems (Strauss *et al.* 2008d). Nevertheless, Bathe (Bathe 1995) suggests a top-down approach starting with the coarsest mesh that will capture the dominant behavior of the physical model: (a) use the simplest elements that will do the job, and (b) never use complicated or special elements unless there is perfect confidence in their use. An iterative refinement in the discretization of the structure with respect to stress or strain concentration areas ensures computational efficiency (Bathe 1995) and finding the optimal sensor locations (Strauss *et al.* 2008d).

One main concern of the influence line- model correction approach is the adaptation of simulation models by incorporating information from monitoring processes. For this adaptation process, the previously discussed aspects of modeling are of great importance. An optimized simulation model that captures the existing behavior of a monitored structure is the basis for a reliable evaluation of the developing monitoring processes, and assessment of code specified service limit states (SLS; e.g., deflections), ultimate limit states (ULS; e.g., bearing capacity), and durability limit states (DLS; e.g., corrosion resistance) (Hoffmann 2008, Strauss *et al.* 2009a,b, Zilch *et al.* 2009, Wendner *et al.* 2010b).

3. Influence line and model correction factor methods

3.1 Influence lines

The structural effects due to specific loads or load combinations can be obtained from the load associated deflection of the influence lines by the following energy based general approach

$$\Sigma W^* = W_a^* + W_i^* = Z_i \cdot \Delta \delta_i + P(x) \cdot w(x) - \int Z \cdot \delta \cdot dx \tag{1}$$

with W_a^* and W_i^* = external and internal work, respectively; Z_i = actual internal force in the entire system due to the force $P = 1$, $\Delta \delta_i$ = virtual mutual deformation of the inserted degree of freedom of the associated mechanical quantity of interest, $w(x)$ = virtual deflection of the influence lines on the
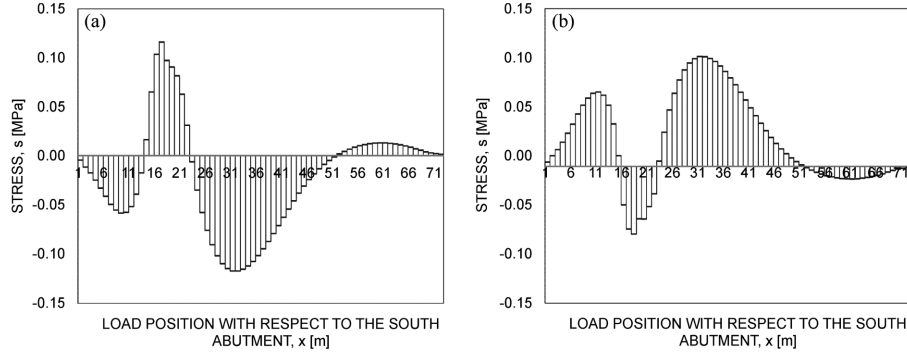
Fig. 1 Numerically generated influence lines (IL) for the three span abutment free bridge S33.24: (a) for stresses associated with the fiber optic strain sensor d_{7u} next to the bottom surface of the slab and loads located in lane 1 according to Fig. 6 and (b) for stresses associated with the fiber optic sensor d_{90o} next to the upper surface of the slab

location and in the direction of P due to $\Delta\delta_i = -1$, and δ = virtual deformation of the entire system due to $\Delta\delta_i = -1$. Eq. (1) yields the following form for statically determinate systems

$$Z_i \cdot \Delta\delta_i + P(x) \cdot w(x) = 0 \tag{2}$$

which is the basis for the following statement by Betti and Maxwell (Hirschfeld 2008). The relationship between Z_i, and $w(x)$ for a moving load $P = 1$ in x is valid as long as the relative displacement in i, $\Delta\delta_i = -1$ is used for the generation of $w(x)$

$$Z_i = w(x) \tag{3}$$

The generalization of this approach for statically indeterminate systems was formulated by Land (Hirschfeld 2008) as follows: The influence line for an internal force Z_i (e.g., N_i, V_i, M_i) in i due to a variable load $P = 1$ in space is equal to the bending line $w(x)$ which is caused by the relative displacement in i, $\Delta\delta_i = -1$ (Δu_i, Δw_i, $\Delta\varphi_i$) at the location of the associated internal force Z_i of interest. Influence lines can be generated numerically (e.g., using the finite element method) by the gradual assignment of the mechanical quantity Z in i due to the unit load $P = 1$. For instance, Figs. 1(a) and 1(b) portray the simulated influence lines obtained by the finite element model presented in Fig. 5(a) along lane 1 (see Fig. 4(a)) for the stresses of the associated sensors d_{7u} and d_{9o}, (see Fig. 4(b)) respectively.

3.1 Model correction factors

In general, an initial model layout for the description of engineering structures will not capture the real behavior due to aleatory and epistemic uncertainties. These uncertainties can be reduced by engineering knowledge. Uncertainties can also be taken into account by model correction factors according to EN1990 Appendix D (2002). The model correction factor based evaluation requires the development of a design model for the theoretical monitored quantity m_t of the member or structural detail considered and represented by the model function

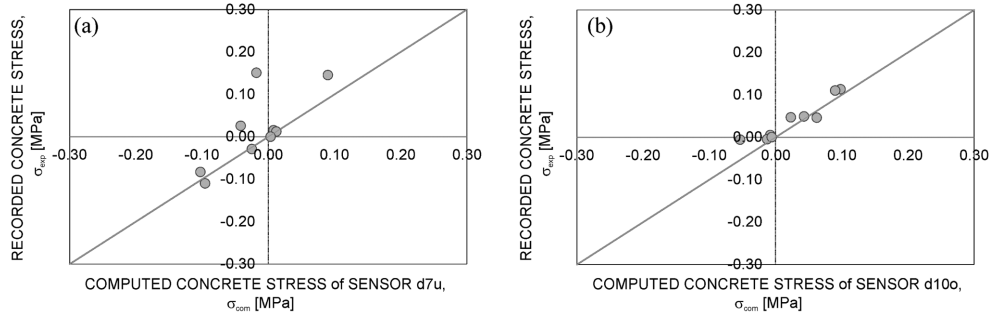$$m_t = g_{mt}(\mathbf{X}) \tag{4}$$

Fig. 2 Recorded and computed stresses of sensor (a) d_{7u} and (b) d_{10o} due to the nine proof loading locations, see Table 3 and Fig. 6, on the S33.24 Bridge

Fig. 3 Case study "Marktwasser Bridge S33.24": (a) Side view - Picture taken from North - East, (b) typical installed fibre optical sensor and (c) vehicles for the proof loading campaign

The model function has to cover all relevant basic variables **X** that affect the design model at the monitoring locations. The basic parameters should be measured or tested. Consequently, there is interest in a comparison between theoretically computed and monitored values. Therefore, the actual measured or tested properties have to be substituted into the design model so as to obtain theoretical values m_{ti} to form the basis for a comparison with the recorded values m_{ei} from a monitoring system. The representation of the corresponding values (m_{ti}, m_{ei}) on a diagram, as shown in Fig. 2 for the recorded and computed stresses due to the nine proof loading locations on the S33.24 bridge, see Fig. 6, allows a pre-assessment of the developed design model. If the design model is exact and complete, then all of the points will lie on the line $\varphi = \pi/4$. In practice the points will show some scatter, as portrayed in Fig. 2. However, the cause of any systematic deviation from that line should be investigated to check whether this indicates errors in the monitoring system or in the design model.

   The estimator of the mean value correction factor represents the appropriateness of the developed model (i.e., the finite element model of the S33.24 shown in Fig. 5). The probabilistic model of the monitored quantity m can be represented in the format

$$m = b \cdot m_t \cdot \delta \tag{5}$$

where b = "Least Squares" best fit to the slope, given by

$$b = \Sigma m_{ei} \cdot m_{ti} / (\Sigma m_{ti} \cdot m_{ti}) \tag{6}$$

In addition, the mean value of the theoretical design model, calculated using the mean values X_m of the basic variables, can be obtained from

$$m_m = b \cdot m_t(X_m) \cdot \delta = b \cdot g_{mt}(X_m) \cdot \delta \tag{7}$$

The error terms δ_i of the recorded values m_{ei} and the paired design model values m_{ti} are given by:

$$\delta_i = m_{ei}/(b \cdot m_{ti}) \tag{8}$$

The logarithm of δ_i

$$\ln(\delta_i) = \Delta_i \tag{9}$$

serves for the computation of the mean value $E(\Delta) = \Delta'$ as

$$\Delta' = 1/n \cdot \Sigma \Delta_i \tag{10}$$

and for the estimation of the variance

$$s_\Delta^2 = 1/(n-1) \cdot \Sigma(\Delta_i - \Delta')^2 \tag{11}$$

which serves for the determination of the coefficient of variation V_δ of the δ_i error terms in the following way:

$$V_\delta = \left(\exp(s_\Delta^2) - 1 \right)^{0.5} \tag{12}$$

In addition to this consideration in the scattering quantities, there is the requirement for a compatibility analysis, in order to check the assumptions made in the design model. If the scatter in (m_{ei}, m_{ti}) values is too high to give realistic design model functions, this scatter may be reduced in one of the following ways: (a) by correcting the design model to take into account parameters which had previously been ignored; (b) by modifying b and V_δ by dividing the recorded test population into appropriate sub sets for which the influence of such additional parameters may be considered to be constant.

4. Case study on the abutment free bridge system S33.24

The jointless "Marktwasser Bridge" S33.24 is a foreshore bridge leading to a recently erected Danube crossing which is part of an important highway connection to and from Vienna. The structure actually consists of two structurally separated bridge objects, the wider one of which allows for five lanes of highway traffic. The S33.24 is a three-span continuous plate structures with span lengths of 19.50 m, 28.05 m and 19.50 m orthogonal to the abutment (20.93 m, 29.75 m, 20.93 m parallel to the main axis) as is shown in Fig. 4(a). The top view of the so called "Marktwasser Bridge", see Fig. 4(a), shows a crossing angle of 74° between center-line of the deck slab and abutment-axis. Further design aspects of this non-prestressed construction are monolithical connections between bridge deck, pillars and abutments as well as haunches going from a constant
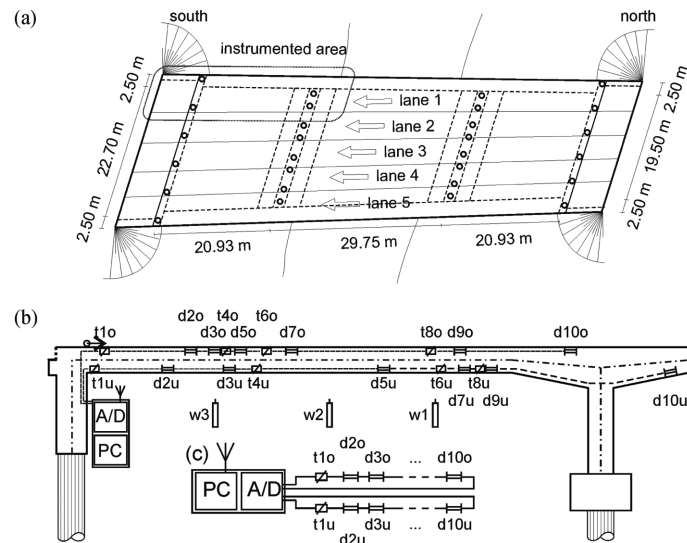
Fig. 4 Monitoring installation plan of the Bridge system S33.24: (a) top view indicating the traffic lanes and instrumented area, (b) longitudinal cut of S33.24 including sensor placement in the deck slab of the southernmost span and (c) serial system topology of fiber optical monitoring system

construction height of 1.00 m to 1.60 m in the vicinity of the pillars to account for the high restraint moment. The deck width ranges from 19.40 m to 22.70 m excluding two cantilevers of 2.50 m length each. The entire structure is founded on four lines of drilling piles with length of 12.00 m and 19.50 m respectively. Further information about the geometry of the structure is given in (Strauss *et al.* 2010). The side view during construction presented in Figs. 3(a) and 3(b) shows one of the fiber optical strain sensors shortly before installation, and Fig. 3(c) presents one of the trucks used during the proof loading campaign.

4.1 Monitoring system

As the design and the performance of abutment free structures depend not only on dead load and the traffic loads but especially on constraint loads resulting from temperature, earth pressure and creep/shrinkage processes an integrative monitoring concept had to be developed covering the superstructure, its interaction with the reinforced earth dam behind the abutment and the dilatation area above the approach slabs. In total 5 different sensor systems consisting of strain gages, temperature sensors and extensometers were permanently installed (Wendner *et al.* 2010b).

Due to the different nature of the relevant load cases the instrumentation of the deck slab had to ensure that both a constant and linear strain distribution across the cross section can be detected. Similarly by a proper placement of the temperature sensors constant temperature and temperature gradient were to be measured (Strauss *et al.* 2010b). Based on those requirements the contractor designing the monitoring system opted for a fiber optic sensor (FOS) system consisting of 12 strain and eight temperature sensors, which were placed in the southern span's deck slab, as shown in Fig. 4(b). For redundancy as well as installation reasons two independent FOS strands were placed in the top and the bottom reinforcement layer of the southern span's deck slab, see Fig. 4(c).

All temperature and strain sensors are equally distributed between upper and lower reinforcement

Table 1 Layout of the fiber optical monitoring system next to the upper and lower surface of the slab of the first lateral field

Sensors	Position [m]	Sensor	Position [m]
t_{1o}	0.70	t_{1u}	0.30
d_{2o}	4.10	d_{2u}	3.15
d_{3o}	5.10	d_{3u}	5.65
t_{4o}	5.10	t_{4u}	6.70
d_{5o}	6.10	d_{5u}	11.70
t_{6o}	7.10	t_{6u}	14.00
d_{7o}	8.10	d_{7u}	14.90
t_{8o}	13.60	t_{8u}	15.70
d_{9o}	14.70	d_{9u}	15.70
d_{10o}	19.10	d_{10u}	23.00
		w_3	5.68
		w_2	10.19
		w_1	14.38

layers. The location of the temperature sensors allows capturing differences in the environmental conditions due to solar radiation, wind and the development of cold air pockets below the deck. Strain sensors d_{2u}, d_{3u} and their counterparts d_{2o} up to d_{7o} provide information about the strain contribution from dead load, creep shrinkage and temperature gradient. The placement of sensors d_{7u}, d_{9u} and d_{9o} was governed by the goal to determine the zero-crossing of the moment distribution whereas d_{10o} and d_{10u} are mainly affected by a constraint moment near the pillar. Table 1 gives a summary of the individual sensor locations, where u denotes bottom reinforcement layer and o denotes upper layer.

4.2 Mechanical model

During design of the monitoring system a 3D finite element model was set up in SOFISTIK in order to (a) optimize the sensor location with respect to the expected structural response and (b) allow for a meaningful data interpretation. The abutments, columns and deck slab were discretized using shell elements. The four rows of drilling piles were modeled by means of beam elements resulting in a total of 569,035 elements and 18,945 nodes. Geometry and material properties were taken out of the initial statics and available plans. Table 2 gives an overview of the used material properties, in particular concrete of class C30/37 for the deck slab, abutments and columns and C25/30 for the piles. In the initial model, see Fig. 5(a), all piles are placed on stiff vertical springs with an initial spring stiffness c_p of 3 GN/m. Horizontally neither the abutment nor the deck slab are supported. The piles are bedded considering a linear increase in the horizontal stiffness modulus from 0 to 40,000 kN/m² at a depth of 5.0 m below the top end of the pile. In the lower area a constant stiffness modulus of the bedding of 60,000 kN/m² is considered.

This initial model was idealized as depicted in Fig. 5(b) with springs of c_p c_{p2} c_{m2} = 3 GN/m vertical stiffness and c_m = 3 GNm/rad rotational stiffness in order to study the influence of the boundary conditions in more detail. This model is referred to later on as Model 2. No
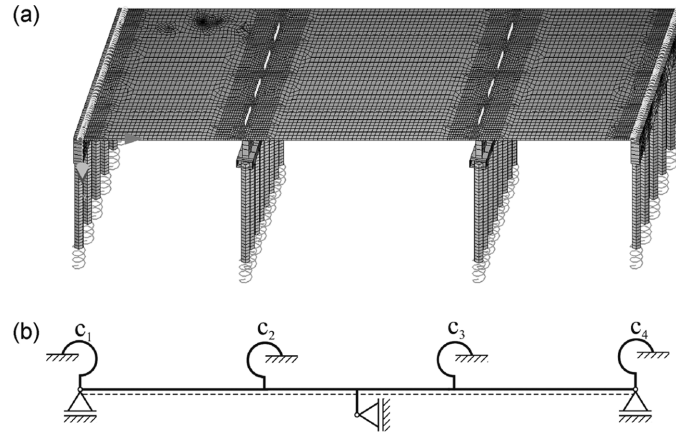
Fig. 5 Numerical models used for the description of the monitored behavior of the Bridge system S33.24: (a) three dimensional linear Finite Element Model incorporating shell (Quads), beam and spring elements and (b) a simplified idealized beam element model representing the modified 3D FEM by spring elements capturing the variability in the stiffness to the abutment (Parameter studies have been performed with $c_1 = c_2 = c_3 = c_4$)

Table 2 Code based material properties of the bridge system S33.24

	Characteristics	Unit	Value
Concrete C30/37	Elastic modulus, E	MPa	31939
	Poisson's ratio, μ	-	0.20
	Shear modulus, G	MPa	13308
	Specific weight, γ	kN/m^3	25
	Coefficient of thermal expansion, α	1/K	1.00E-05
Concrete C25/30	Elastic modulus, E	MPa	30472
	Poisson's ratio, μ	-	0.20
	Shear modulus, G	MPa	12696
	Specific weight, γ	kN/m^3	25
	Coefficient of thermal expansion, α	1/K	1.00E-05
Reinforcment BST 550	Elastic modulus, E	MPa	210000
	Poisson's ratio, μ	-	0.30
	Shear modulus, G	MPa	80769
	Specific weight, γ	kN/m^3	78.5
	Coefficient of thermal expansion, α	1/K	1.20E-05

differentiations were made between the springs at the abutment axes c_1 and c_4 and the column axes c_2 and c_3 respectively. For Model 1 the stiffness of all springs was reduced by a factor of three to $c_{p1} = 1$ GNm/rad and $c_{m1} = 1$ GNm/rad whereas for Model 3 the stiffness was increased by a factor of three to $c_{p3} = 9$ GN/m and $c_{m3} = 9$ GNm/rad respectively.

4.3 Proof loading procedure (PLP)

Proof load tests have been performed on Friday, Feb. 19th 2010 between 10:50 a.m. and 14:45 pm
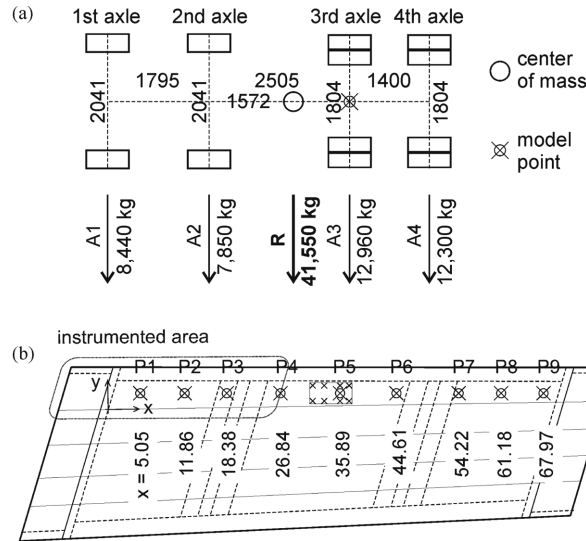
Fig. 6 Proof loading associated details: (a) Geometrical configuration and axle load distribution of the proof loading vehicles and (b) static proof loading positions of the vehicles along lane 1 of the bridge system S33.24

with ambient temperatures between $0°$ to $2\,°C$. The results of these proof loadings serve for the calibration of the static linear model and the verification of the assumed structural behavior. The concept for the proof loading procedure was developed with the following goals in mind. Firstly defined load situations with significant structural response were to ensure a proper model calibration mainly with respect to the boundary conditions. As a consequence three 40 to trucks with known axle loads were positioned in 16 static scenarios. The trucks were positioned independently as well as in the most unfavorable configurations on lanes 1 to 3, see Fig. 4(a).

Furthermore dynamic effects and the respective amplification factor should be determined to ensure a proper interpretation of real traffic load effects on the overall performance. To that end in total 35 load scenarios with moving vehicles from walking pace to a speed of approximately 50 km/h were performed.

For the model calibration nine static load situations with a single truck of 41.55 to in lane 1 were considered only. The trucks axle configuration and axle load distribution resulting from deadload and freight is presented in Fig. 6(a). Fig. 6(b) illustrates the load positions with respect to the model point in chosen local coordinates. The stepwise moving along the bridge axis results in an experimental determination of the influence lines for all sensor properties and sensor positions respectively which provide great insight into the system behavior.

4.4 Numerical representation of PLP

The main goal as already mentioned previously is the assessment of the validity and adequacy of the initial numerical model to be used during future structural performance assessment. To that end, the predicted structural response is compared to the real response recorded by the monitoring system for clearly defined load situations.

This model validation is, in particular, for abutment free bridge structures essential. Due to the

nature of these structures and the still limited knowledge several significant assumptions regarding (a) the soil-structure-interaction, (b) the influence of temperature effects, and (c) the stiffness distribution within the structure have to be made during design.

For example, the effects of deformations and nonlinear material laws are not being considered in the initial finite element model for the determination of the internal forces. Furthermore, the stiffness distribution, which in case of reinforced concrete structures is variable due to the development of micro cracks (between the uncracked state I and the fully cracked state II), is not considered either. These significantly influence structural response, especially in a statically indeterminate structure, where constrained loads and force redistribution govern performance. Within this contribution the model validation includes, on the global level, a direct comparison of structural response between real structure and model. On the local level, observed stress/strain distributions in individual structural members (e.g., deck slab) are checked against the original design calculations.

The influence line concept in combination with the proof-loading procedure allows a simplified comparison based on short-term relative measurement data instead of absolute values, which are influenced by long-term processes and initial offset. Only the nine load situations P_i with trucks positioned according to Fig. 6(b) are considered. Due to the limited duration of the proof loading campaign, the effects of creep, shrinkage, changes in temperature and settlement on the monitored quantities can be neglected, thus yielding the basis for an unbiased comparison.

The actual model validation is based on a comparison of the expected values of the monitored quantities $E(\mathbf{m}_{ei}) = (\overline{m}_{ei,1}, \overline{m}_{ei,2}, \ldots, \overline{m}_{ei,n})$ for the n sensors and $i = 1,..,9$ proof loading positions with the expected values of the respective simulated quantities $E(\mathbf{m}_{ti}) = (\overline{m}_{ti,1}, \overline{m}_{ti,2}, \ldots, \overline{m}_{ti,n})$. In both cases, influence lines are obtained by plotting the expectations against the load positions.

The agreement between model and reality can be expressed in terms of the model correction factor b. If the numerical model can fully capture the real loading situation, resistance and accurately represent structural response, then a perfect model would be present, indicated by $b = 1$. Furthermore the characteristic response m_k according can be calculated.

For the case study object S33.24 virtual proof loadings using the axle load configuration of the truck presented in Fig. 6(a) have been simulated. The center of mass was positioned in the first lane and moved in increments of 1.00 m yielding the simulated expectations $E(\mathbf{m}_{ti})$ for strains related to the fiber optic strain sensors $d_{2o}, d_{3o}, d_{5o}, d_{7o}, d_{9o}, d_{10o}$ which are located in the top reinforcement layer, and $d_{2u}, d_{3u}, d_{5u}, d_{7u}, d_{9u}, d_{10u}$ which are located in the bottom reinforcement and for the vertical deflections related to the LVDT sensors $w_1,\ldots,w_3$. Since mean values are used to describe the material properties in the models, the simulated influence lines for the respective sensors are directly obtained by plotting the resulting simulated expectations against the load positions, see exemplarily Figs. 7 and 8.

On a global level, the model validity can be checked by comparing the global structural response of the real structure with e.g., the initial finite element model in terms of the influence line values.

If, for the majority of available sensors, the shape of the simulated continuous influence lines shows a good agreement with the measured discrete influence line values, the assumed load transfer mechanism can be confirmed. Figs. 7 and 8 illustrate this comparison in terms of the sensors d_{9o} d_{7u}, w_1, and w_2. Although the black columns (measurement) generally follow the shape of the theoretical influence lines, deviations in absolute values as well as e.g., the position of the zero crossings are present with respect to the different numerical models. These discrepancies can be used to (a) efficiently identify inaccuracies in the individual models, and (b) finally choose the model with the highest agreement.
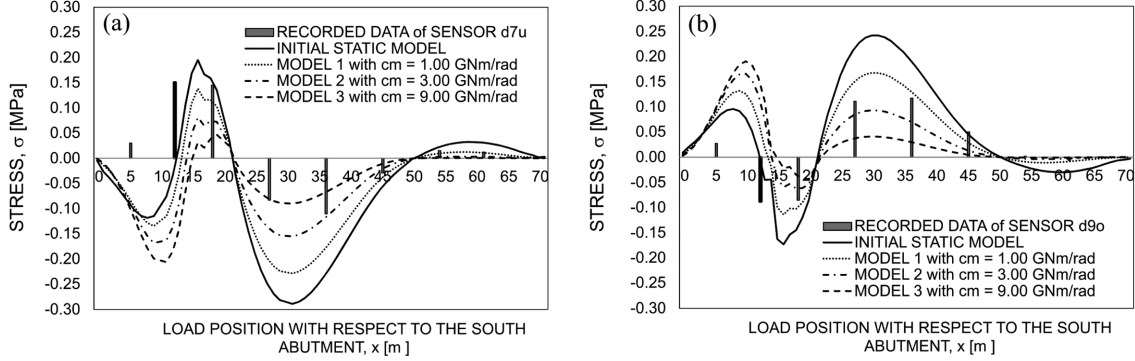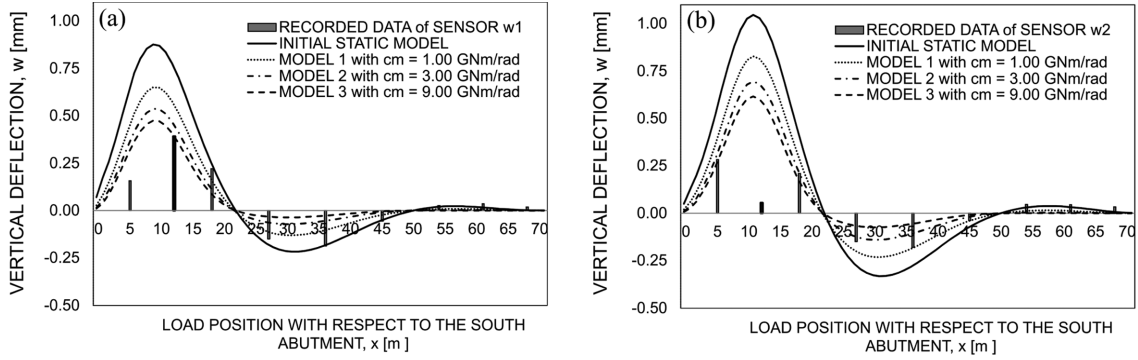
Fig. 7 Influence lines (IL) extracted from the Finite Element Model of the bridge system S33.24 (Fig. 5(a)) with respect to the measured values of the nine proof loading positions: (a) IL of stresses associated with the fiber optical sensor d_{7u} and (b) IL of stresses associated with the fiber optical sensor d_{9o}

Fig. 8 Influence lines (IL) extracted from the Finite Element Model of the bridge system S33.24 (Fig. 5(a)) with respect to the measured values of the nine proof loading positions: (a) IL of vertical deflections associated with the LVDT sensor w_1 and (b) IL of vertical deflections associated with the LVDT sensor w_2

In addition to a qualitative comparison between models and reality based on the shape of the measured and simulated influence lines, the available influence values can also be used to quantitatively assess the deformation (deflection) and load bearing (strain) behavior of (a) the northern, (b) the middle, and (c) the southern span. For a given sensor i the average deviation Δm_i for n discrete load positions is obtained by

$$\Delta m_i = [(m_{ti} - m_{ei})_{P1} + \ldots + (m_{ti} - m_{ei})_{Pn}]/n \tag{13}$$

For example, the discrete measured influence line values related to the strain sensors d_{7u} and d_{9o} show for the proof loading positions P_7 to P_9 located in the *northern span* deviations of $\Delta m_{d7u} = +1.15\%$ and $\Delta m_{d9o} = -1.38\%$ with respect to the simulated quantities for the initial model, see Fig. 7. The deviations related to the deflection influence line values of sensors w_1 and w_2 amount to $\Delta m_{w1} = -1.43\%$ bzw. $\Delta m_{w2} = -1.82\%$, see Fig. 8.

The observed discrepancies are mainly caused by simplifications associated with the initial linear model and assumptions regarding the boundary conditions (e.g., bedding of drilling piles). In particular, the analysis of measured and simulated influence lines based on the initial linear model reveals a

systematic error $B_{FOS,P7-P9}$ = -0.0012·X for the fiber optic sensors and $B_{LVDT,P7-P9}$ = -0.0163·X for the LVDT monitoring system. In a first approach, the modification of the boundary conditions in terms of the rotational spring stiffness for the support axes allows a minimization of the residuals (see dashed lines in Figs. 7 and 8). However, due to structural and mechanical nonlinearities (e.g., load-dependent micro cracks lead to changes in stiffness) the deviations generally cannot reach zero.

For the proof loading positions P_4 to P_6 located in the *main span*, an average deviation of Δm_{d7u} = -10.77% and Δm_{d9o} = +5.92% for the strain sensors (Fig. 7) and Δm_{w1} = -0.82% and Δm_{w2} = -8.61% (Fig. 8) for the LVDT monitoring system can be obtained. Considering the shape of the simulated influence lines according Figs. 7(a) and 7(b) a reduction in deviations for the fiber optic monitoring system can be reached by assuming an effective rotational spring stiffness of c_m = 3.00 GNm/rad - in a first approach abutment walls and columns have been substituted by idealized translational and rotational springs, see Fig. 5(b). An effective reduction of the respective residuals for the LVDT sensors is only possible for a significantly smaller rotational spring stiffness of $c_m \sim 1.00$ GNm/rad as compared to the initial model.

For the main span, overall the initial finite element model shows, a stiffer response than the real structure exhibits.

The systematic error associated with the fiber optic sensors and loads positioned in the main span can, at average, be expressed by $B_{FOS,P4-P6}$ = -0.0243·X with regard to the initial linear model and $B_{LVDT,P4-P6}$ = -0.0472·X, respectively for the LVDT system.

For the *southern span* the influence values associated with sensors d_{7u} and d_{9o} and proof loading positions P_1 to P_3 show an average deviation of Δm_{d7u} = -29.55% and Δm_{d9o} = +12.51% with regard to the simulations, see Fig. 7. According to Fig. 8 for sensors w_1 and w_2 the deviations amount to Δm_{w1} = -14.64% and Δm_{w2} = +28.87%, respectively. Furthermore, both sensor systems seem to indicate a systematic shift as compared to the theoretical influence lines. The resulting systematic error may be quantified for the southern span by $B_{FOS,P1-P3}$ = -0.0852·X and $B_{LVDT,P1-P3}$ = +1.0712·X. The simplified model N°3 with a rotational spring stiffness of c_{m3} = 9.00 GNm/rad would allow a reduction of the observed deviations, thus suggesting a too soft behavior of the initial model in the southern span.

In addition to the global comparison of structural response between numerical models and real behavior based on the proposed influence line approach, 2D and 3D nonlinear finite element analyses (ATENA, Červenka *et al.* 2007) have been performed in order to study *localized effects*.

These detail investigations reveal the following additional sources for deviations between simulated and measured strains: The initial as well as the simplified linear finite element models are not able to accurately capture the real strain/stress trajectories. In particular, (micro) cracks and the reinforcement layout locally affect the strain/stress trajectories, which also partially cause the observed shift between measured and simulated influence line values. Furthermore, active (loads) and passive (boundaries) contributions to the real strain/stress trajectories caused by the soil-structure-interaction (e.g., variable effects of the earth pressure against the abutments) as well as temperature loads, dead load and traffic loads cannot be fully captured by the investigated numerical models.

The evaluation of the LVDT monitoring data is, apart from the above mentioned effects, mainly influenced by the variable stiffness distribution in the deck slab due to micro-cracking (transition from linear elastic to nonlinear elastic), that cannot be accounted for in the linear model.

Finally, a combined investigation of the individual, partially redundant monitoring systems together with nonlinear finite element analysis has been performed in order to exclude the following reasons
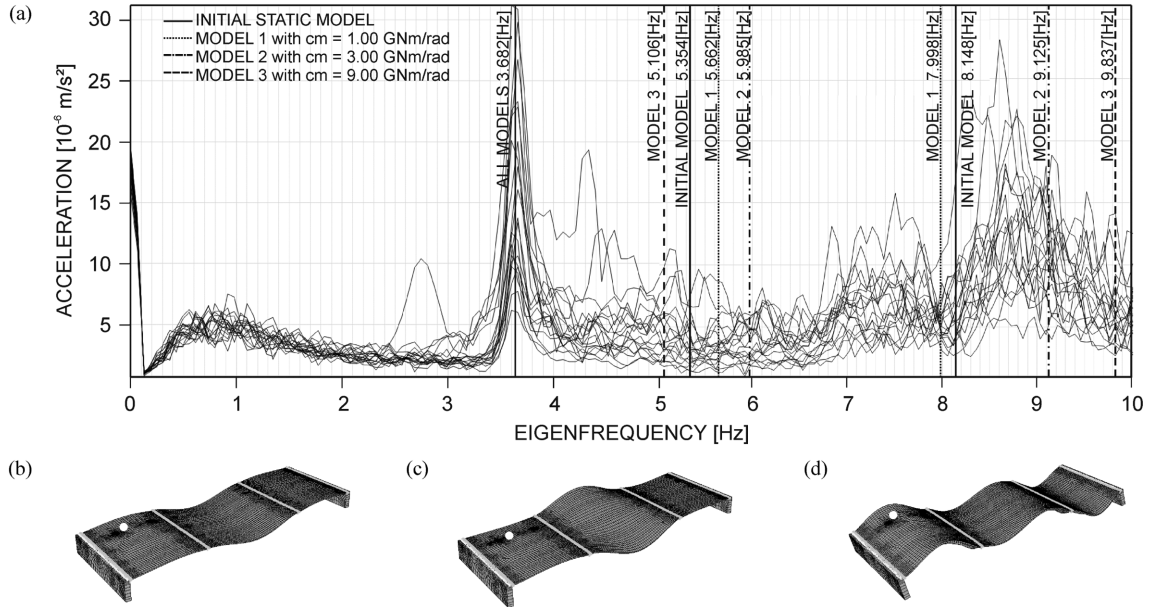
Fig. 9 (a) Measured spectrum vs. lower eigenfrequencies obtained for the initial and the simplified finite element models N° 1 to 3, see Fig. 5. Mode shapes of (b) 1st, (c) 2nd and (d) 3rd natural frequency of Model N° 1
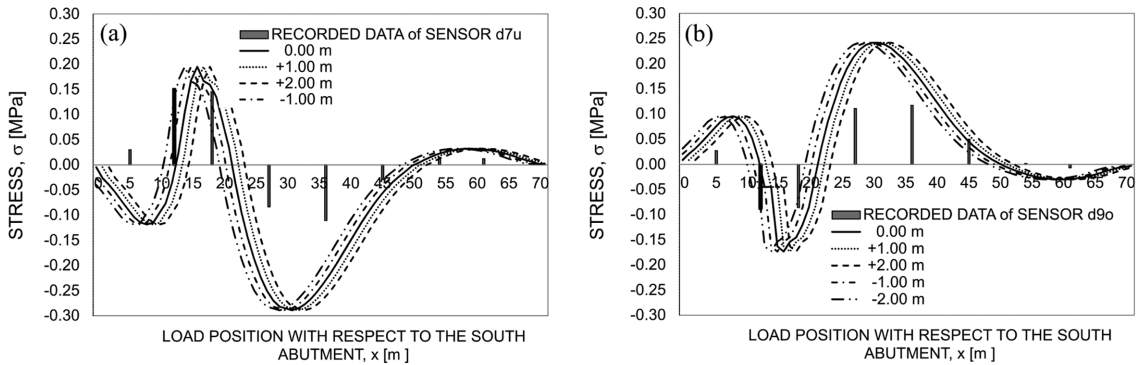

Fig. 10 Influence lines (IL) extracted from the Finite Element Model of the bridge system S33.24 (Fig. 5(a)) with respect to the measured values of the nine proof loading positions: (a) IL of stresses associated with the fiber optical sensor d_{7u} and (b) IL of stresses associated with the fiber optical sensor d_{9o}

for deviations: (a) inaccurately documented truck positions during the proof loading procedure (Fig. 10 shows the influence line studies for shifted proof load positions), (b) insufficiently calibrated monitoring systems, and (c) effects on the strain/stress trajectories caused by the haunches near the column axes.

4.5 Assessment of measured frequencies with respect to calculated ones

In addition, to the traditional local monitoring methods, global monitoring concepts can be applied which open up further possibilities for model adaptation as well as a verification of the

local monitoring results. During the proof loading procedure two accelerometers were placed in midspan of the southern span and the main span respectively. Fig. 9 shows the experimental frequency spectrum derived from repeated measurements at site using a fast fourier transform (FFT) with respect to the numerically generated eigenfrequencies for all four models considered. This representation places the first numerically derived eigenfrequency at 3.682 Hz, the second numerically derived eigenfrequency between 5.106 and 5.985 Hz and the third numerically derived eigenfrequency between 7.998 and 9.837 Hz, depending on the respective degree of restraint to the bridge base.

The results and measured values outlined above show that a model adaptation for this structure by global monitoring information (e.g., first eigenfrequencies) is very difficult due to (a) the low sensitivity of the first eigenfrequency to changes in the structural system, (b) the fact, that the second natural frequency is associated with the torsion mode in midspan and thus cannot be captured experimentally by the accelerometer in the first field, see Fig. 9, and (c) the large by scattering contaminated range of the third eigenfrequency, which is a combined flexural-torsional mode. It must be noted, that the large scattering in the experimental spectrum is in all likelihood be caused by spatial effects in the plate system and the small energy content associated with ambient vibration.

4.6 Quantification of goodness of fit

The quantitative comparison of the numerically derived influence line values with the measured values (see previous section) facilitates, (see Fig. 11), an efficient evaluation of modeling concepts and sensor data sensitivity. Fig. 11 represents a five-class evaluation of the agreement of the measured values with the numerically derived model values of the sensor properties for the proof loadings. It presents the four numerical models that differ in their degree of restraint with respect to the supporting structure. In particular, it shows the evaluation of the influence line values for the measured values of the fiber-optical monitoring system without correction factors. It emerges that the best agreement is achieved (a) considering solely the fiber-optical sensor system for the Model N°2 (e.g., highest number of class evaluation ≤ 3.0), and (b) considering the deflection monitoring system only for the initial model.
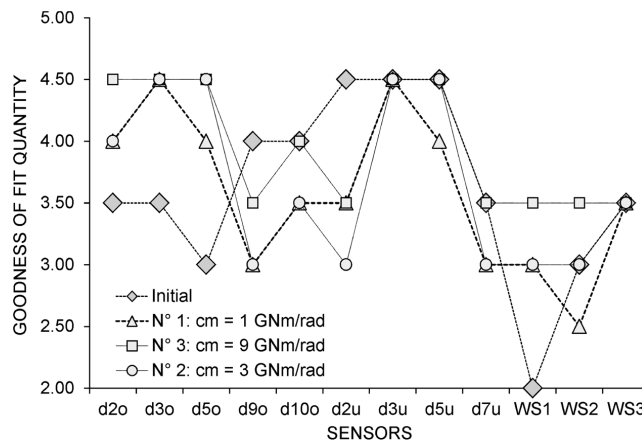

Fig. 11 Subjectively assessed goodness of fit quantities

4.7 Quantification of goodness of fit – model correction factor approach

A more analytical and statistically based procedure for the quantification of the agreement between numerically generated influence lines and experimentally obtained influence value is provided by the model correction factor concept, as presented in Eqs. (9) to (27). The model correction factor allows (a) the assessment of the model behavior with respect to the real structural response, (b) the assessment of the time variable structural performance due to degrading processes based on sensor data, and (c) a limit state analysis with respect to code given requirements. The simulated and recorded sensor characteristics for all nine load positions associated with the proof loading of the bridge system S33.24 serve for the computation of the model correction factor b. Fig. 12 portrays the mean value correction factors of the previously discussed simulated and measured influence line values associated with the nine proof loading positions. The individual b-values can be summarized with respect to (a) the goodness of fit of an individual model, (b) the capability of an entire monitoring system to represent a certain structural characteristic, or (c) to evaluate single sensors. In that context, an average quadratic deviation from the perfect fit ($b_{sys} = 1$) is proposed as system indicator, as follows

$$b_{sys} = 1 - \frac{1}{n}\sqrt{\sum_{i=1}^{n}(1 - b_i)^2} \qquad (14)$$

From the representations in Fig. 12, it follows that the initial model may be interpreted as statistically suitable with system indicators $b_{sys} = 0.57$ for the FOS in the upper layer, $b_{sys} = 0.71$ for the FOS in the bottom layer and $b_{sys} = 0.44$ for the LVDT sensors measuring the vertical deflection. The more flexible Model N°1 in general is the more suitable model with $b_{sys} = 0.64$ for the FOS in the upper layer, $b_{sys} = 0.54$ for the FOS in the bottom layer and $b_{sys} = 0.69$ for the LVDT sensors. In agreement with JCSS a spectrum of values ranging from 0.60 to 1.40 is acceptable due to aleatory and epistemic uncertainties (Vrouwenvelder 1997, 2001).

Going from a positive shift of the computed influence lines to a shift equal -3.0 m the agreement
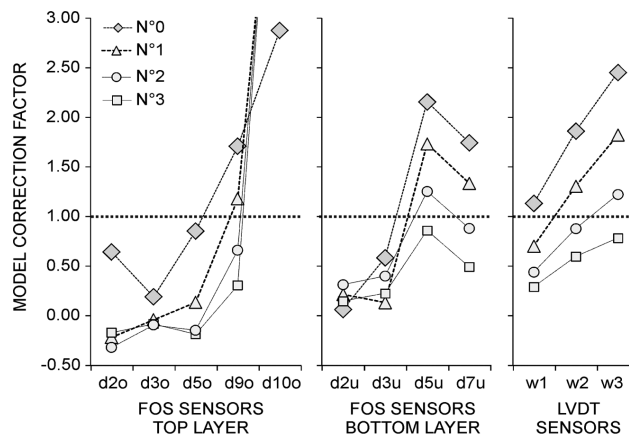

Fig. 12 Model correction factors associated with the fiber optical and LVDT sensor systems: N°0 = initial model; N°1 = model with c_m = 1 GNm/rad; N°2 = model with c_m = 3 GNm/rad; and N°3 = model with c_m = 9 GNm/rad

between model and monitoring data gradually increases from $b_{sys} = 0.55$ to $b_{sys} = 0.88$, when only the 4 analyzed sensors (d_{7u}, d_{9o}, w_1, w_2) are considered. Although an obvious trend can be identified for the system indicator b_{sys}, no such trend is present for any of the model correction factor b_i associated with individual sensors. The lack of an optimum within the investigated feasible range of a horizontal shift in the load position indicates that no systematic error is present in the available monitoring data that affects all sensors equally. However, the proposed concept based on the influence line and model correction factor concept would have been able to identify this type of error.

5. Conclusions

1. The influence-line model correction approach has been theoretically presented and combined into an efficient procedure for the incorporation of monitoring data in the modeling and subsequently assessing the performance of existing structures. In particular, the proposed approach was applied to the three span abutment free bridge system S33.24, which has been instrumented with fiber optical sensors, a LVDT and an ambient vibration monitoring system.
2. The investigation of the influence line- model correction approach, using monitoring and simulation information, shows its ability to efficiently identify the comprehensive load transfer and bearing behavior of an engineering system.
3. The model correction part of the proposed approach provides a statistical quantification of the agreement between a descriptive simulation model and the monitored structural behavior.
4. The model correction approach is not restricted to a single sensors but can be applied to a group of sensors of an individual monitoring system and even to a group of monitoring systems.
5. The influence line- model correction approach separately applied to the lateral and middle fields of the abutment free bridge S33.24 revealed that the chosen linear simulation model is not able to completely capture the true structural behavior due to geometrical and material nonlinearities. The mean value correction factors are indicators for deficiencies in the current model. These indicators can be considered as objectives to be optimized in the course of a model updating procedure (Hoffmann *et al*. 2007, Movák and Lehký 2006, Strauss *et al.* 2004). Furthermore, probabilistic sensitivity analyses techniques with respect to these indicators can serve for the detection of those structural and material parameters, which cause the ill conditioned indicators. Finally, this knowledge allows a rational approach in the adaptation of descriptive models by the refinement in the geometry or in material properties of the initial model and even in the selection of advanced simulation techniques (e.g., two dimensional or three dimensional nonlinear simulation techniques).

The influence line approach has been performed for the fiber optical sensor- and for the LVDT-monitoring system. Despite the great potential in acquiring information regarding the real stress/strain state at given locations the fiber optical strain sensors, did not show that good results as the LVDT measurements for the linear design model. These deviations may result from (a) the sensor location and its bond to the reinforcement (e.g., the measured strains might directly reflect steel strain, concrete strain or something in between in case of an already cracked cross-section), and (b) the principal strain stress direction which is not necessarily aligned with the sensor direction.

The presented approach combining the influence line concept with the model correction factor concept for the incorporation of monitoring data into modeling concepts does not only provide the basis for efficient and objective model updating strategies but also is essential for the performance assessment of structures over time.

Acknowledgements

References

Bathe, K.J. (1995), *Finite-Element-Method*, Springer.
Bergmeister, K. and Wendner, R., Wörner, J.D. and Fingerloos, F. (2010), "Monitoring und Strukturidentifikation von Betonbrücken", *Betonkalender*, **1**, 245-290.
Červenka, V., Jendele, L. and Červenka, J. (2007), *ATENA Program Documentation, Part I*, Theorie. Prague, Czech Republic.
Doebling, S.W., Farrar, C.R., Prime, M.B. and Shevitz, D.W. (1996), *Damage identification and health monitoring of structural and mechanical systems from changes in their vibration characteristics: a literature review*, Los Alamos National Laboratory.
Dorvash, S., Yao, R., Pakzad, S. and Okaly, K. (2010), "Static and dynamic model validation and damage detection using wireless sensor networks", *Proceedings of the 5th international conference on bridge maintenance, safety and management IABMAS2010*, D.M. Frangopol, R. Sause and C.S. Kusko. Philadelphia, Pennsylvania, USA, Taylor & Francis Group, London, 1282-1286 (on CD-ROM).
Eurocode - Basis of structural design (2002), EN 1990. Brüssel, Belgium, European Committee for Standarization.
Frangopol, D.M. (2011), "Life-cycle performance, management, and optimization of structural systems under uncertainty: accomplishments and challenges", *Struct. Infrastruct. E.*, **7**(6), 389-413.
Frangopol, D.M. and Okasha, N.M. (2008), "Life-cycle performance and redundancy of structures", *Proceedings of the 6th Int. Probabilistic Workshop*, C.A. Graubner, H. Schmidt and D. Proske. Technische Universität, Darmstadt, Germany, 1-14.
Frangopol, D.M., Strauss, A. and Kim, S. (2008a), "Use of monitoring extreme data for the performance prediction of structures: General approach", *Eng. Struct.* **30**(12), 3644-3653.
Frangopol, D.M., Strauss, A. and Kim, S. (2008b), "Bridge reliability assessment based on monitoring", *J. Bridge Eng.*, **13**(3), 258-270.
Geier, R. (2010), "The benefit of monitoring for bridge maintenance", *Proceedings of the 5th international conference on bridge maintenance, safety and management IABMAS2010*, D.M. Frangopol, R. Sause and C. S. Kusko. Philadelphia, Pennsylvania, USA, Taylor & Francis Group, London: 415-422(on CD-ROM).
Hirschfeld, K. (2008), *Baustatik Theorie und Beispiele*, Berlin Heidelberg New York, Springer.
Hoffmann, S. (2008), *System identification by directly measured influence lines - A user orientated approach for global damage identification at reinforced concrete bridges*. Wien, Universität für Bodenkultur. Dissertation: 149.
Hoffmann, S., Wendner, R., Strauss, A., Ralbovsky, M. and Bergmeister, K. (2007), "AIFIT–anwenderorientierte identifikation für Ingenieurtragwerke, versuchsgestützte steifigkeitsanalysen", *Betonund Stahlbetonbau*, **102**(10), 699-706.
Inaudi, D. (2010), "Optimal design of bridge SHM systems based on risk and opportunity analysis", *Proceedings of the 5th international conference on bridge maintenance, safety and management IABMAS2010*, D.M. Frangopol, R. Sause and C.S. Kusko. Philadelphia, Pennsylvania, USA, Taylor & Francis Group, London: 2119-2126 (on CD-ROM).
Kim, S. and Frangopol, D.M. (2010), "Optimal planning of structural performance monitoring based on reliability assessment", *Probab. Eng. Mech.*, **25**(1), 86-98.
Kim, S. and Frangopol, D.M. (2011a), "Cost-effective lifetime structural health monitoring based on availability", *J. Struct. Eng.*, **137**(1), 22-33.
Kim, S. and Frangopol, D.M. (2011b), "Cost-based optimum scheduling of inspection and monitoring for

fatiguesensitive structures under uncertainty", *J. Struct. Eng-ASCE*, **137**(11).

Kwon, K. and Frangopol, D.M. (2010), "Bridge fatigue reliability assessment using probability density functions based on field monitoring data", *Int. J. Fatigue*, **32**(8), 1221-1232.

Liu, M., Frangopol, D.M. and Kim, S. (2009a), "Bridge system performance assessment from structural health monitoring: a case study", *J. Struct. Eng-ASCE*, **135**(6), 733-742.

Liu, M., Frangopol, D.M. and Kim, S. (2009b), "Bridge safety evaluation based on monitored live load effects", *J. Bridge Eng.*, **14**(4), 257-269.

Liu, M., Frangopol, D.M. and Kwon, K. (2010a), "Fatigue reliability assessment of retrofitted steel bridges integrating monitoring data", *Struct. Saf.*, **32**(1), 77-89.

Liu, M., Frangopol, D.M. and Kwon, K. (2010b), "Optimization of retrofitting distortion-induced fatigue cracking of steel bridges using monitored data under uncertainty", *Eng. Struct.*, **32**(11), 3467-3477.

Mayr, M. and Thalhofer, U. (1993), Numerische Lösungsverfahren in der Praxis: FEM-BEM-FDM, Hanser.

Messervey, T.B. and Frangopol, D.M. (2009), "Life-cycle cost and performance prediction: role of structural health monitoring", Frontier Technologies for Infrastructures Engineering. S.S. Chen and A.H.S. Ang. Leiden, The Netherlands, CRC Press-Balkema-Taylor & Francis Group: 361-381.

Messervey, T.B., Frangopol, D.M. and Casciati, S. (2010), "Application of statistics of extremes to the reliability assessment of monitored highway bridges", *Struct. Infrastruct. E.*, **7**(1-2), 87-99.

Novák, D. and Lehký, D. (2006), "ANN inverse analysis based on stochastic small-sample training set simulation", *Eng. Apl. Artif. Intel.*, **19**(7), 731-740.

Orcesi, A.D. and Frangopol, D.M. (2010a), "Inclusion of crawl tests and long-term health monitoring in bridge serviceability analysis", *J. Bridge Eng.*, **15**(3), 312-326.

Orcesi, A.D. and Frangopol, D.M. (2010b), "Optimization of bridge management under budget constraints: Role of structural health monitoring", *Transportation Research Record: Journal of the Transportation Research Board (Bridge Engineering 2010: Volumes 1-3)*, **3**(2202), 148-158.

Orcesi, A.D. and Frangopol, D.M. (2011), "Optimization of bridge maintenance strategies based on structural health monitoring information", *Struct. Saf.*, **33**(1), 26-41.

Orcesi, A.D., Frangopol, D.M. and Kim, S. (2010), "Optimization of bridge maintenance strategies based on multiple limit states and monitoring", *Eng. Struct.*, **32**(3), 627-640.

RVS 13.03.11, "Monitoring von Brücken und anderen Ingenieurbauwerken", *Überwachung, Kontrolle und Prüfung von Kunstbauten - Straßenbrücken*.

Strauss, A., Bergmeister, K., Novák, D. and Lehký, D. (2004), "Stochastische parameteridentifikation bei konstruktionsbeton für die betonerhaltung", *Beton- und Stahlbetonbau*, **99**(12), 967-975.

Strauss, A., Bergmeister, K., Wendner, R. and Hoffmann, S. (2009a), "System- und Schadensidentifikation von Betonstrukturen", *Betonkalender*, **2**, 55-125.

Strauss, A., Frangopol, D.M. and Kim, S. (2008c), "Use of monitoring extreme data for the performance prediction of structures: Bayesian updating", *Eng. Struct.*, **30**(12), 3654-3666.

Strauss, A., Frangopol, D.M. and Kim, S. (2008d), "Statistical, probabilistic and decision analysis aspects related to the efficient use of structural monitoring systems", *Beton- und Stahlbetonbau*, **103**(S1), 23-28.

Strauss, A., Hoffmann, S., Wendner, R. and Bergmeister, K. (2009b), "Structural assessment and reliability analysis for existing engineering structures, applications for real structures", *Struct. Infrastruct. E.*, **5**(4), 277-286.

Strauss, A., Wendner, R., Bergmeister, K. and Frangopol, D.M. (2010a), "Monitoring based analysis of an concrete frame bridge Marktwasser bridge", *Proceedings of the 3rd International fib Congress*, Washington, DC, USA.

Strauss, A., Wendner, R., Bergmeister, K. and Frangopol, D.M. (2011), "Monitoring and influence lines based performance indicators", *ICASP 11 Applications of Statistics and Probability in Civil Engineering*, M. Faber, J. Köhler and K. Nishijma. Zurich, Switzerland: 1059-1068.

Strauss, A., Wendner, R., Bergmeister, K. and Horvatits, J. (2011), "Modellkorrekturfaktoren als "Performance Indikatoren", für die Langzeitbewertung der integralen Marktwasserbrücke S33.24", *Beton- und Stahlbetonbau*, **106**(4), 231-240.

Strauss, A., Wendner, R., Bergmeister, K. and Reiterer, M. (2010), "Monitoringbasierte analyse von integralen brücken am beispiel der marktwasserbrücke", *Schriftenreihe des Departments*, K. Bergmeister. Vienna, Department für Bautechnik und Naturgefahren, Universität für Bodenkultur. 20.

Vrouwenvelder, T. (1997), "The JCSS probabilistic model code", *Struct. Saf.*, **19**(3), 245-251.

Wendner, R., Strauss, A., Bergmeister, K. and Frangopol, D.M. (2010b), "Monitoring based evaluation of design criteria for concrete frame bridges", *IABSE Symposium 2010*, Venice, Italy.

Wendner, R., Strauss, A., Guggenberger, T., Bergmeister, K. and Teplý, B. (2010), "Ansatz zur beurteilung von chloridbelasteten stahlbetonbauwerken mit bewertung der restlebensdauer", *Beton- und Stahlbetonbau*, **105**(12), 778-786.

Wenzel, H. and Egerer, V. (2010), Determination of a performance baseline for lifecycle consideration of bridges, *Proceedings of the 5th international conference on bridge maintenance, safety and management IABMAS2010*, D.M. Frangopol, R. Sause and C.S. Kusko. Philadelphia, Pennsylvania, USA, Taylor & Francis Group, London: 1282-1286 (on CD-ROM).

Zilch, K., Weiher, H., Gläser, C., Bergmeister, K., Fingerloos, F. and J.D. Wörner. (2009), "Monitoring im betonbau", *Betonkalender*, 2.

JCSS Probabilistic Model Code Part 1: Basis of Design (2001).

FC